Materials Advances

ROYAL SOCIETY OF CHEMISTRY

REVIEW

View Article Online
View Journal | View Issue

Cite this: *Mater. Adv.*, 2026, 7, 715

The role of atomic-level understanding in optimizing lithium titanate oxide based anodes for lithium-ion batteries

Emaan Shahid and Abdul Majid *

Lithium titanate oxide (LTO) has gained significant attention recently as a promising candidate for anode materials in lithium-ion batteries because of its stable operating potential and unique zero-strain behavior. Despite these advantages, its use is limited because of poor electronic conductivity and sluggish lithium-ion diffusion. This review highlights how the atomic-level understanding of various strategies, such as structural architecture engineering, doping, and defect engineering, is gained through advanced computational approaches. Computational studies on lithium vacancies and defects reveal how dopants like Nb^{5+} and Al^{3+} influence the charge transport and introduce charge compensation. Furthermore, density functional theory (DFT) based studies illustrate that the diffusion barrier of lithium ions at engineered sites is significantly lower than that of the bulk structure. The impact of these three modification strategies on the LTO structure is examined along with experimental validation of the computational results. Finally, this review highlights future directions of the role of computational tools in accelerating the performance and rational design of high-performance LTO anodes.

Received 8th September 2025,
Accepted 14th November 2025

DOI: 10.1039/d5ma01027f

rsc.li/materials-advances

1. Introduction

The global imperative of transitioning to a suitable energy economy and reducing carbon emissions has solidified the position of lithium-ion batteries, making them essential for everything from electric cars to phones and large-scale power grids.[1,2] As the lithium-ion battery market continues its rapid expansion, the demand for batteries that last longer, can store more energy, and are safer is increasing.[3,4] The anode is a key component in battery performance as it directly impacts the key metrics such as rate capability, capacity, and operational safety.[5,6] For several decades, graphite has been the governing anode material due to its low cost, reasonable specific capacity ($\sim$372 mAh g^{-1}), and stable intercalation chemistry.[7–9] However, several limitations of graphite anodes limit their use in next-generation high-energy lithium-ion batteries.[10] Graphite has a low operating voltage (<0.2 *vs.* Li/Li^+), which is below the typical electrochemical stability window for carbonate-based electrolytes, resulting in the formation of a dynamic and fragile solid electrolyte interphase (SEI) that contributes to capacity decay due to its consumption of active lithium.[11–13] More critically, the dendrite formation at low temperatures and high charge rates is caused by the non-uniform deposition of metallic lithium on the anode surface. These dendrites can penetrate the separator and can lead to thermal runaway due to an internal short circuit. The major motivation behind an alternative anode material is the safety concern faced by the circuit. High energy density is also one of the main and rising demands that is fueling further research. Lithium metal and silicon are the widely used anode materials, but lithium metal suffers from safety issues and silicon faces a volume expansion of about 300%; all such kinds of issues emphasize the need for an anode material that overcomes these issues and has extraordinary performance.[14–16]

Lithium titanate oxide (LTO) has gained considerable attention due to its zero-strain behavior, in this regard. It undergoes a structural two-phase transition from the cubic spinel phase to a rock-salt phase during the lithiation process.[17] During this transition, the stoichiometry changes from $Li_4Ti_5O_{12}$ to $Li_7Ti_5O_{12}$, accompanied by a minor volume change (less than 1%) that enables an exceptionally long life cycle (often surpassing 10 000 cycles) and remarkable structural stability.[18–20] These features make LTO-based batteries more durable and inherently safer than their graphite counterparts. Fig. 1 illustrates the conversion of spinel $Li_4Ti_5O_{12}$ to its rock salt form, $Li_7Ti_5O_{12}$, through the lithiation process.

However, the broad implementation of LTO is hindered by two main intrinsic limitations. Firstly, pristine LTO exhibits relatively low theoretical capacity ($\sim$175 mAh g^{-1}), restricting the overall energy density of the battery cell.[22,23] Secondly, it

Department of Physics, University of Gujrat, Gujrat 50700, Pakistan.
E-mail: abdulmajid40@yahoo.com

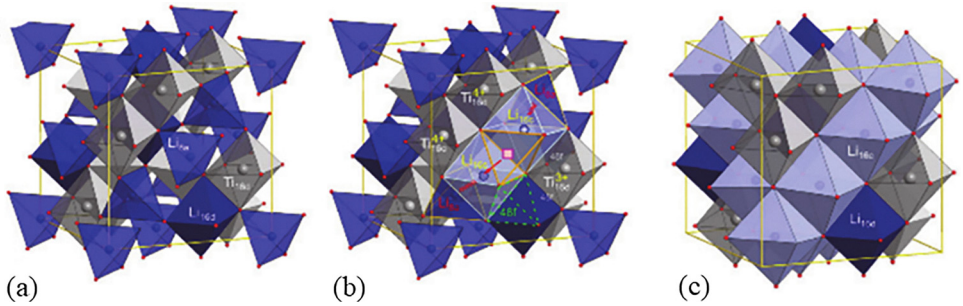

Fig. 1 (a) Spinel-type $Li_4Ti_5O_{12}$. (b) Structural changes. (c) $Li_7Ti_5O_{12}$. Reprinted with permission from open access.[21]

exhibits insulating behavior with a wide bandgap and low Li-ion diffusivity, resulting in poor ionic and electrical conductivity.[24] This low conductivity hinders the charging speed and rate capability, reducing its suitability for high-power applications such as electric vehicles. Understanding of a material at the atomic level is very important for studying its limitations and possible solutions, which is not possible through experimental studies alone. Density functional theory (DFT) based calculations offer effective ways to understand such materials and behaviors.[25]

The main aim of this review is to provide a better understanding of the limitations of LTO as an anode and possible solutions to these limitations through various strategies, such as structural architecture engineering, doping and defect engineering, through first-principles and DFT simulations and studies.[26,27] This will provide a deeper understanding of the behavior and electronic properties of the material under different strategic conditions. The second strategy is strategic doping. It explains how the deliberate introduction of foreign atoms, both anions and cations, can be considered as an advanced form of defect engineering.[28] Through the substitution of titanium or lithium into the spinel framework, dopants are shown to effectively modulate the electronic bandgap, modify its working potential, and alter the lithium-ion diffusion pathway to reduce the migration barrier significantly.[29] Fig. 2 presents some of the drawbacks of the LTO anode and their possible solutions through some key strategies such as doping, defect engineering, and structural architecture engineering.

This fine-tuning at the atomic level presents a promising strategy for optimizing the electrochemical performance of LTO by directly addressing its intrinsic conductivity limitations.[30] The third strategy analyzed in this review is structural architecture engineering. Unlike the previous two methods, it focuses on the physical modification of LTO. It investigates the profound impact of nano-structuring (nanosheets and nanoparticles) along with surface chemistry and interfacial engineering on charge transport behavior and transfer kinetics.[31] It highlights how increasing the electrochemically active surface area and reducing diffusion lengths can markedly improve rate capability, providing a crucial complement to atomic-level enhancements introduced through such structural modifications.[32,33] By consolidating the mechanistic insights from these comprehensive methods and investigations, a high-level perspective emerges that bridges experimental and theoretical findings. This integrated understanding offers an atomic-scale design roadmap to engineer advanced high-performance next-generation LTO anode materials, providing strategic guidance to accelerate future development and research in this field.

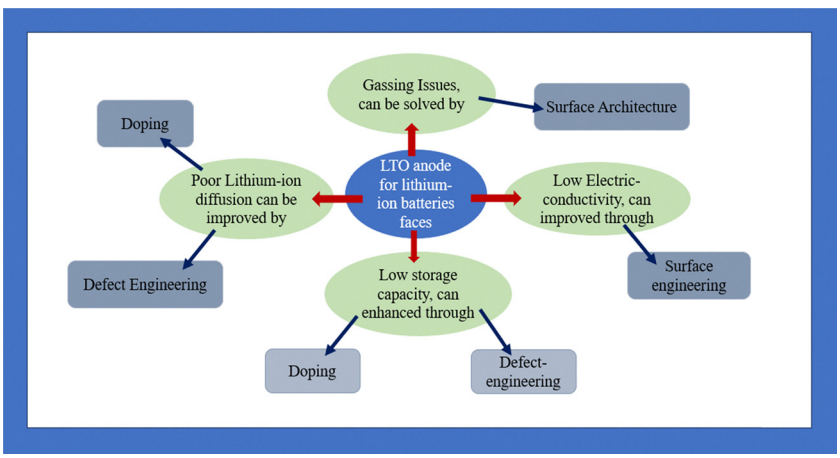

Fig. 2 Visual representation of issues faced by the LTO anode and the expected solutions.

2. Computational framework

The majority of first-principles investigations on lithium-ion battery materials, such as LTO, are based on DFT.[30] DFT represents a powerful quantum mechanical approach that enables the study of the electronic structure of a system without the need to solve complex many-body Schrödinger equations.[34] Its foundation lies in the Hohenberg–Kohn theorems, which predict that the ground-state electron density of a system uniquely determines its properties.[35] This allows the many-body problem to be simplified into a more manageable set of single-body equations.[36,37] The solution of these equations provides the electron density of the system, which helps yield the total energy and other critical properties of the system. In practical applications, the accuracy of DFT depends on approximations for the exchange–correlation functional, which approximates the quantum mechanical interaction among the electrons. The most commonly employed approximation are the generalized gradient approximation (GGA) and local density approximation (LDA), along with the Perdew–Burke–Ernzerhof (PBE) functional being widely adopted within the GGA family.[38] These functionals are very popular in describing many material systems, but often face challenges in modeling the systems with strongly localized electrons, such as in transition metal oxides like LTO.[39,40]

Modeling of LTO faces distinct challenges due to the presence of titanium atoms with partially filled d-orbitals, which leads to electron correlation, a phenomenon of strong electron–electron repulsion. The standard GGA functional often fails to accurately capture this localization, leading to a significant underestimation of the bandgap and a misrepresentation of the electronic structure.[41] To correct this deficiency, a DFT+U approach is widely employed as a corrective method.[42] This semi-empirical method adds an on-site Hubbard U parameter into the Hamiltonian, which effectively penalizes the double occupancy of localized d-orbitals and corrects the self-interaction error inherent in conventional DFT.[43]

The bandgap of LTO was predicted to be 1.5 eV using the standard GGA parameter. This severe underestimation was corrected by using the Hubbard U parameter of about 4.5 eV for the 3d orbitals of Ti, through which the values of E_g got aligned with the experimental value of 3.6 eV. For a specific kind of limitation, various kinds of doping are a promising strategy to overcome this by promoting the Ti^{3+} or Ti^{4+} mixed values. On the other hand, studies have also proved that the best stability and mitigating gassing are best achieved through surface coating or atomic layer deposition of Al_2O_3 or ZrO_2. For LTO, the appropriate selection of the U parameter for titanium d-states is paramount for obtaining accurate electronic and structural properties.[44] The computational modeling for LTO simulations requires meticulous attention to ensure reliable and meaningful results. To study defects and dopants, a supercell is constructed as an expanded version of the unit cell, and its size must be large enough to reduce artificial interactions among the defect periodic images, usually containing 56 atoms or more.[45] The critical factor in evaluating the rate capability of LTO is the identification of the energy barrier, which involves identifying the energy barriers of lithium ions, precisely done using the NEB method. The NEB method is the most accurate tool for this purpose, as it determines the minimum energy path and saddle point from which the migration energy barrier can be governed, providing valuable insight into ionic conductivity.[46,47] Beyond migration studies, DFT enables a range of calculations for essential properties, including the electronic density of states (DOS), dopant and defect formation energies, and the average working potential of the anode is obtained by comparing the total energies of lithiated and delithiated phases.[48] Table 1 summarizes the DFT functionals used to study different-sized supercells of LTO, along with the key properties investigated in these studies.

In the case of LTO, atomic-level insights primarily from MD and DFT simulations, guided the material optimization methods, replacing the trial-and-error methods. Initial DFT calculations accurately identify the rate-limiting step for the diffusion of lithium ions as the one with a high energy barrier of approximately 0.6 eV for the ionic movement.[49,50] The computational screening has prescribed the use of low concentration dopants such as Al^{3+} and Mg^{2+}, which were calculated to reduce the local strain, further verified by the experimental studies that optimized synthesis routes, achieving 10^{-3} cm^2 s^{-1} to 10^{-2} cm^2 s^{-1}, confirming the structural and model design.[51] The DFT+U is very efficient in diagnosing the limitations regarding the conductivity of LTO by confirming the presence of Ti^{3+} polarons and a process to track the charge transport. This atomic-level diagnosis regarding the LTO/electrolyte interface mandated a shift in experimental focus towards its betterment through techniques such as defect creation and doping, which are able to stabilize and enhance the material.[16]

3. Methodological advantages and limitations

DFT excels at providing exceptional atomic-level insights and predictive capability enabling rapid material screening and

Table 1 Common DFT settings and functionals used in LTO studies

No.	DFT functional	Hubbard U for Ti (eV)	K-point sampling	Supercell size (atoms)	Key property investigated	Ref.
1	PBE	—	5 × 5 × 5	14	Lithium diffusion pathway	52
2	PBE+U	2.7	2 × 2 × 2	56	Intrinsic defects and conductivity	53
3	PBE sol+U	2.8	2 × 2 × 2	168	Anion doping	54
4	PBE sol+U	2.5	3 × 3 × 3	112	Cation doping	55
5	PBE+U	2.6	4 × 4 × 4	56	Surface effects on Li	56
6	PBE+U	2.9	3 × 3 × 3	224	Nano-structure properties	55
7	GGA+U	3.0	2 × 2 × 2	112	Co-doping strategies	56

supporting exceptional synthesis of LTO. It has played a dominant role in quantifying the reduction in the Li-ion migration barrier due to doping and elucidating surface reactivity mechanisms.[57] However, the accuracy of DFT depends crucially on the chosen Hubbard *U* parameter and exchange correlation functional, resulting in significant variability in reported values.[58] As a ground-state and static method, it struggles with capturing complex, time-dependent phenomena like extensive diffusion or SEI formation, which demand more computationally intensive techniques such as *ab initio* molecular dynamics (AIMD), underscoring the importance and need for rigorous methodological validations and choices through experimental data.[59]

4. Intrinsic defects in $Li_4Ti_5O_{12}$ anodes

The presence of native point defects profoundly influences the fundamental properties of any crystalline material, including diffusivity and ionic conductivity.[60] These defects, emerging from thermodynamic equilibrium during synthesis or battery operation, play a crucial role in critically determining the electrochemical performance of the LIB electrode material.[61] In the case of pristine LTO, understanding the nature and concentration of these intrinsic defects is essential for elucidating its inherent limitations and developing strategies to improve performance.[62]

4.1. Defect formation

In the spinel structure of LTO, a variety of intrinsic point defects can exist, each influencing the material properties differently. Among the most commonly investigated are lithium vacancies (V_{li}), oxygen vacancies (V_O), and antisite defects, especially lithium-titanate antisite (Li_{Ti}) and titanium-lithium antisite (Ti_{Li}).[63,64] Although interstitial defects like oxygen (O_i) and lithium (Li_i) are theoretically feasible, their higher formation energies under standard conditions generally render them relatively rare.[65]

DFT calculations are indispensable for evaluating the formation energies of these defects in varying chemical potential environments and across varying Fermi levels.[66] Lower formation energy corresponds to a higher equilibrium concentration of a defect. Table 2 presents a summary of different kinds of defects in the LTO anode and their formation energies, along with their effect on band gaps. The defects in which the lithium sublattice is involved, such as lithium vacancies (V_{Li}) and lithium-titanium antisites, have the lowest values of formation energies, 0.1 to 0.5 and 0.2 to 0.7, respectively. These lower values of formation energies represent the stability and equilibrium of the defective structures of LTO anodes. This indicates that Li^+ disorder is thermodynamically favorable as the intrinsic disorder for the spinel LTO anode structure, as it makes the movement of Li^+ ions within the structure much easier.[67] On the other hand, the formation energy value of V_O is in the range of 1.5 to 3.0 eV, which is a higher value that is considered considerable only in high-temperature synthesis or in a reducing atmosphere for creating highly conductive LTO anode materials.[68] Moreover, the intermediate value of formation energy for titanium-lithium antisites (T_{Li}) which is 0.8–1.5 eV, confirms the local structural stability and potentially hinders a long lithium diffusion pathway.[69] Defect concentrations are highly sensitive to synthesis conditions such as oxygen partial pressure and temperature, which DFT accurately simulates through chemical potentials.[70] Fig. 3(a′) presents various types of defects created in the structure of $Li_4Ti_5O_{12}$ and the effects on structural atoms due to these defects and local structural distortions that influence the Li ion pathway.

To understand the defect characteristics and intrinsic stability of LTO, the formation energies of various defects created in the material are presented in Fig. 3(b′). In this plot, the formation energies of all six defects from A to F are plotted against the equilibrium conditions, which represent the limits of chemical potential illustrated by the existence of specific competing phases. The phase boundaries of (A) Li_2TiO_3, (B) TiO_2, (C) Li_2O, (D) $Li_2Ti_3O_7$, (E) Ti_2O_3, and (F) $LiTiO_2$ represents the stability limit of LTO for various chemical potential conditions. The analysis indicates that under lithium-rich conditions, such as under condition C for Li_2O, the formation energies for lithium interstitials (Li_i) and lithium vacancies (V_{Li}) are relatively low, indicating the preference for lithium-related defects. On the other hand, the titanium-related defects (V_{Ti}) are less likely to form across the equilibrium condition because they are highly energetic. So, the antisite defects are considered as the most favorable among A to C, according to the existing understanding of the LTO structure, and suggesting that the minor mixing of Li or Ti is the dominant defect mechanism. These equilibrium conditions are also considered crucial because they define the chemical potentials μ_{Li}, μ_{Ti}, and μ_O of the constituent elements, and they are related to the

Table 2 Summary of key defects in LTO

No.	Defect type	Formation energy (eV)	Effect on the bandgap	Electronic impact	Ionic impact	Ref.
1	Oxygen vacancy (V_O)	1.5–3.0	Creates mid-gap due to Ti^{3+} states	Enhances electronic conductivity	Influences the local Li environment	76
2	Lithium vacancy (V_{Li})	0.1–0.5	Introduces acceptor states near the valence band	Negligible electronic activity	Facilitates diffusion	77
3	Titanium-lithium antisite (Ti_{Li})	0.8–1.5	Creates mid-gap due to Ti^{3+} states	Negligible electronic activity	Can block the Li diffusion pathway	78
4	Lithium-titanate antisite (Li_{Ti})	0.2–0.7	Introduces deeper acceptor states	Enhances electronic conductivity	Hinders Li diffusion	79

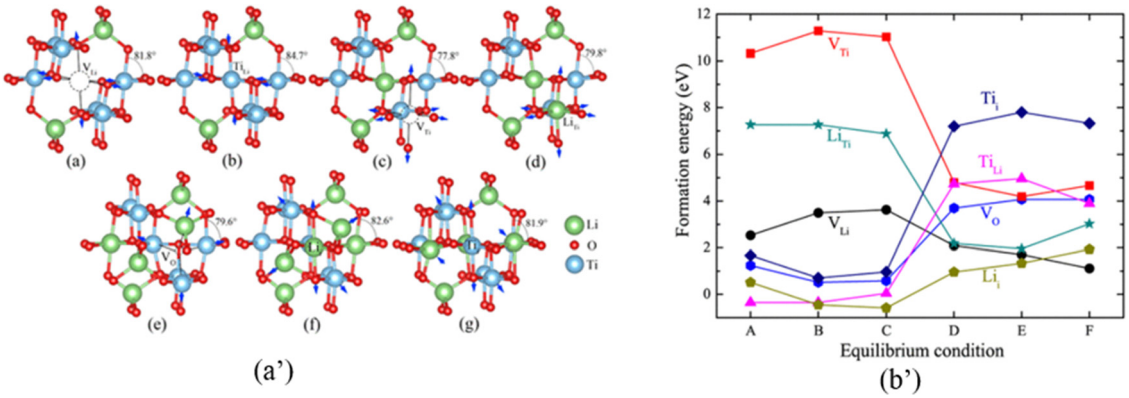

Fig. 3 (a'), (a) V_{Li}, (b) T_{Li}, (c) V_{Ti}, (d) Li_{Ti}, (e) V_O, (f) Li_i, and (g) Ti_i. Relaxation directions of atoms are represented by blue arrows, and vacant spaces from where the atoms are removed are shown by dashed circles. (b') The formation energies for the defect created LTO structure under equilibrium conditions. Reprinted with permission from American Chemical Society.[66]

phase boundaries to play their role in preventing the precipitation of secondary phases. μ_{Li} is reduced in the case of V_{Li}, which results in their increased energies and helps in determining the most favorable defects for the LTO structure.

4.2. Electronic properties

Intrinsic defects significantly modify the electronic structure of LTO, a critical factor in influencing the electronic conductivity. In its pristine stoichiometric form, LTO is considered an insulator with a wide band gap ($\sim$3.5 eV), primarily due to fully occupied t_{2g} and empty e_g orbitals of Ti^{4+}. However, the introduction of defects can create localized states in this bandgap, effectively reducing the activation energy for electronic transport.[71,72] For instance, V_O often triggers the formation of Ti^{3+} ions in its vicinity as a charge compensation mechanism. These Ti^{3+} states introduce electron polarons which are capable of hopping between adjacent titanium sites, thereby enhancing the material's electronic conductivity.[73] Similarly, Li_{Ti} can also generate Ti^{3+} species, contributing to electronic conduction and other electronic properties.[65] The effect of defect creation in LTO is discussed in Table 2; the V_O and Li_{Ti} enhance conductivity as Ti^{3+} localized states are created with these defects within the structure. Such states are referred to as mid-gap states because they are positioned just below the conduction band. On the other hand, the highly prevalent Li_{Ti} and V_{Li} only introduce deep and shallow acceptor states near the valence band, so the primary function remains electronic instead of being structural and ionic. DFT calculations, specifically through analysis of the electronic DOS and band structure, have clearly shown that these defect-induced mid-gap states play a vital role in altering LTO from an insulator with a wide bandgap to a semiconductor.[74] The defect engineering is also performed experimentally, where the creation of oxygen vacancies is proved to be purposeful through EPR spectra, which enable the quantification of paramagnetic Ti^{3+} defects that reduce the lithium migration activation energy, a result obtained using GITT, which indicates a Li-ion diffusion coefficient increase compared to the stoichiometric benchmark.[28,75]

4.3. Electrochemical correlation

The DFT analysis of the impact of various types of defects in the structure of LTO anodes is discussed in Table 2. But these DFT predicted values also have their electrochemical correlation. Most critical types of defects are those which introduce n-type electronegativity such as V_O and Ti_L; both of these defects are charge compensated by the localized reduction of titanium, which causes bandgap narrowing and acts as quantitative underpinning for enhanced conductivity which directly correlates with experimentally observed values of conductivity enhancement of about $\sim 10^{-13}$ to $\sim 10^{-9}$ S cm^{-1} reported for LTO having defects in its structure, overcoming the limitation of rate performance.[80] The conductivity is enhanced up to 10^{-7} S cm^{-1} and it is further verified by impedance spectroscopy, which verifies the role of predicted polaron states. On the other hand, most of the formation energies lie in the region of 2 to 4 eV, which causes discrepancies among the experimentally predicted values using techniques like TGA and XPS analyses.[81,82] Hence, theoretical and experimental results complement each other.[66]

5. Strategic doping for better performance

By substituting host atoms with foreign elements, the lattice structure can be modified, the lithium-ion diffusion pathways optimized, and the electronic band structure adjusted.[83] First-principles calculations have played a vital role in predicting the most promising dopants and revealing the underlying mechanisms, providing the rational basis for experimental work. The primary objectives of doping are to enhance the intrinsic ionic and electronic conductivity, improve specific capacity, and potentially increase the rate capability of LTO.[28,84]

5.1. Cation doping

The substitution of host cations, Li^+ and Ti^{4+}, with foreign metal ions is the most extensively investigated doping approach. The effectiveness of a dopant depends on factors such as its ionic

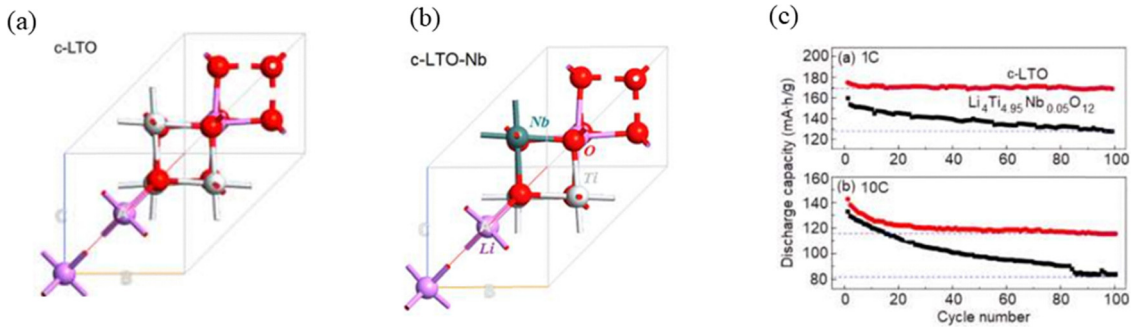

Fig. 4 (a) Atomic structure of c-LTO. (b) Atomic structure of c-LTO-Nb. (c) Cyclic characteristics of c-LTO and c-LTO-Nb. Reprinted with permission from open access.[91]

radius and its preferred substitution site within the lattice.[84] Aliovalent dopants have a different ionic state from the host structure they replace, so they are considered particularly effective as they can successfully alter the electronic properties by introducing charge carriers (electrons or holes).[31] For instance, pentavalent dopants like tantalum (Ta^{5+}) and niobium (Nb^{5+}) are widely used for enhancing electronic conductivity. Fig. 4(a) and (b) present the atomic structure of c-LTO and the doping of niobium into the LTO structure, respectively. Fig. 4(c) shows that the charge rate and reversible capability of c-LTO-Nb are higher than those of c-LTO. It is 135 mAh g^{-1} at 1C and 127 mAh g^{-1} at 20C.[52]

The conductivity of doped LTO also increases, as c-LTO exhibits a conductivity of 6.615×10^{-10} S cm^{-1}, and it improves to 1.127×10^{-9} after doping of niobium into[85] the structure. According to DFT studies, these kinds of dopants reside at Ti^{4+} sites. The substitution is a charge compensation process for another Ti^{4+} to Ti^{3+}, which releases free electrons.[86] These released free electrons are delocalized and reside near the conduction band minimum, significantly narrowing the band-gap and enhancing the electronic conductivity.[87] The trivalent dopants, such as aluminium (Al^{3+}), also reside as substituents at Ti^{4+} sites. The substitution makes a main contribution to reinforcing the structural stability of the LTO lattice. This enhanced stability improves long-term durability by reducing volume changes during cycling.[88] Isovalent dopants such as tin (Sn^{4+}) and zirconium (Zr^{4+}), having the same charge as the Ti^{4+} ion that they replace, do not directly affect the charge balance, so they do not increase the electronic conductivity. Instead, larger ionic radii than Ti^{4+} expand the lattice, which has been predicted computationally to reduce the activation energy for Li-ion hopping. Ionic conductivity is enhanced through this strain-induced modification without compromising LTO's insulating properties.[89,90]

5.2. Anion doping

Anion doping, specifically the replacement of oxygen ions with other elements, is not common but an emerging strategy.[92] The potential of fluorine (F) to enhance the electrochemical properties of LTO has been explored through DFT studies. Replacement of F^{-} with O^{-2} causes a positive charge imbalance that is compensated by the formation of lithium interstitials or oxygen vacancies.[90,92,93] This can modify both the local diffusion environment and the electronic structure of LTO. Strong binding interactions that may also affect Li-ion transport result from the high electronegativity of fluorine. The computational literature on anion doping still suggests that it needs further research.[94]

5.3. Co-doping

To explore further enhancements in properties of LTO, recent computational studies have begun to explore co-doping strategies, in which two different dopants are introduced simultaneously.[95] It aims to combine the positive effects of one dopant, such as electronic conductivity, with the benefits of others. DFT is used to understand the complex effect of the dopants on various properties of the material, such as lithium-ion diffusion and other electronic properties. Table 3 shows different kinds of doping in LTO and their respective impacts on material performance.

5.4. Quantitative assessment of doping strategies

Table 3 summarizes various types of doping performed on LTO to improve its transport kinetics and other properties, such as electronic bandgap (E_g) and lithium ion migration barrier (E_{aLi}). The quantitative data compiled in this table reveal that cation dopants like Nb^{5+} and Ta^{5+} act like dual-function enhancers. Replacing Nb^{5+} or Ta^{5+} with Ti^{4+} introduces a localized positive charge, which is then compensated by either the reduction of Ti^{3+} to Ti^{4+} or by a higher concentration of mobile lithium vacancies. In the case of introduction of aliovalent and isovalent dopants into LTO, the electrostatic perturbation weakens the bond between O^{-2} and Li^{+}, leading to almost 10–25% decrease in migration barrier of such materials. In the same way, the introduction of Ti^{3+} species causes new mid-gap donor states to result in band-gap shrinkage of up to 1.0 eV for Ta^{5+}, leading to the resultant band-gap of about 3.5 eV. This causes the conduction mechanism to shift towards more efficient small polaron hopping. When observed experimentally, the UV-V bandgap measured is almost 2.94 eV, proving that both kinds of studies have related results. The same is the case of the diffusion barrier, when measured for Nb-doped LTO, it is 0.4 eV, which is supported by GITT measurements by showing

Table 3 Summary of doping strategies of $Li_4Ti_5O_{12}$

No.	Dopant	Suitable site	$\Delta E_{a,Li}$ (%)	ΔE_g (%)	Key predicted effects	Stability	Ref.
1	Ta^{5+} (aliovalent)	16d (Ti^{4+})	−15 to −25	−0.5 to −1	Reduces bandgap, enhances electronic conductivity	Highly stabilizing, strong suppression of Ti/Li disorder	86,98
2	Nb^{5+} (aliovalent)	16d (Ti^{4+})	−10 to −20	−0.3 to −8	Reduces bandgap, enhances electronic conductivity, and small lattice expansion	Strongly stabilizing, enhances the thermal stability of the structure	33,99
3	Al^{3+}	16d (Ti^{4+})	+5 to −10	~0.0	Does not affect electronic conductivity	Moderate stability, ensures zero-strain mechanism	100,101
4	Zr^{4+} (isovalent)	16d (Ti^{4+})	0.0 to −5	~0.0	Induces lattice strain and minimal change to electronic properties	Moderate stability	102,103
5	F^- (aliovalent)	32e (Ti^{4+})	−5 to −15	−0.1 to −0.3	May alter the diffusion path	Enhanced integrity, maintains the spinel structure	104,105
6	Al/Nb	16d (Ti^{4+})	−20 to −30	−0.8 to −1.2	Balances structural stability and electronic conductivity	Synergistic stabilization, long term structural integrity	28,106

an increase in the Li-ion diffusion coefficient from 10^{-12} to 10^{-10} cm^2 s^{-1}.[83,86] On the other hand, lower valent dopants show a very negligible change in band gap and act as structural stabilizers, and also offer a migration barrier relief by minor lattice expansion. This quantitative analysis shows that a decrease in migration barrier and lower E_g are effective for better rate capability of doped LTO. The doping with aliovalent ions is often confirmed by EPR and XPS studies, providing evidence of the formation of Ti^{3+} species, which are crucial for enhancing the electronic conductivity and proving the effectiveness of the doping strategy.[96] Electrochemical impedance spectroscopy (EIS) further shows increased lithium ion diffusion coefficients as compared to the pristine structure.[97]

6. Structural architecture and nano-engineering

Surface architecture and nano-engineering are some of the widely used techniques for performance enhancement of the LTO anode material. In other techniques, various external materials are added, or some of the material atoms are removed, but in this technique, only by modifying the surface of the material structure or converting the bulk structure into any other form, such as nano-sheets or thin-films, the material's performance can be enhanced to a greater extent. Various computational studies have already been performed on LTO with a structural architecture applied to it. DFT investigations have meticulously compared various LTO surface facets, such as the more reactive (110) and low-energy (111) planes, to elucidate their roles in lithium-ion diffusion and insertion.[107,108]

Fig. 5 shows a significant effect of surface architecture on the performance of LTO. It illustrates calculated voltage profiles of LTO nanoparticles having (1 0 0), (1 1 0), and (1 1 1) crystal facets, respectively. The different curves for each surface demonstrate that voltage and capacity during lithium insertion are directly influenced by the atomic-level surface geometry of the material. Red and black curves show the presence and absence of neighbouring atoms at the interface, respectively.[110] This shows that the surrounding environment of the material is important in determining the diffusion barrier and activation energy.[111] One of the key findings is that, diffusion barrier of the bulk material is less than the surface, whereas the activation energy at the surface is noted to be lower than that of the bulk. The increased surface-to-volume ratio within the nanomaterials causes faster diffusion and hence results in better rate performance. Advanced computational simulations play a vital role in a better understanding of these strategic processes.

Doping, which has also been discussed in the previous sections, is also considered to be a kind of structural modification, but if compared with nano-engineering, both have their own benefits and limitations.[112] Nano-engineering is good at improving rate performance, whereas doping is suited for enhancing the electronic conductivity of LTO, but these effects are interconnected. Doping enhances the charge transfer. When aliovalent dopants are introduced into the LTO structure, they create charge-compensating Ti^{3+} species for this.[113] As doping enhances the charge transfer, nano-engineering is crucial for improving the rate capability. For the betterment of rate capability, nano-engineering the path length of Li-ion solid-state diffusion also improves the electrolyte–electrolyte contact area.[114] Reducing the Li-ion diffusion path is the best way for fast charge–discharge cycles at high C-rates. So we can say that if we combine doping with nano-engineering in the case of LTO, the best results in terms of performance and properties can be attained.

6.1. Interfaces in composites and all-solid-state materials

The combination of LTO with other conductive components can further enhance its performance as an anode.[115] DFT modeling allows for the investigation of interfacial charge transfer, which can significantly alter the electronic properties of LTO near the contact region.[116,117] These models demonstrate that a strong electronic coupling, resulting from a work function mismatch between LTO and graphene, can reduce the overall interfacial resistance, thereby enabling faster electron transport.[118] The structural stability of the interface is another critical factor, as maintaining robust interfacial bonding is crucial for maintaining structural integrity during repeated lithiation and delithiation cycles. In addition to carbon

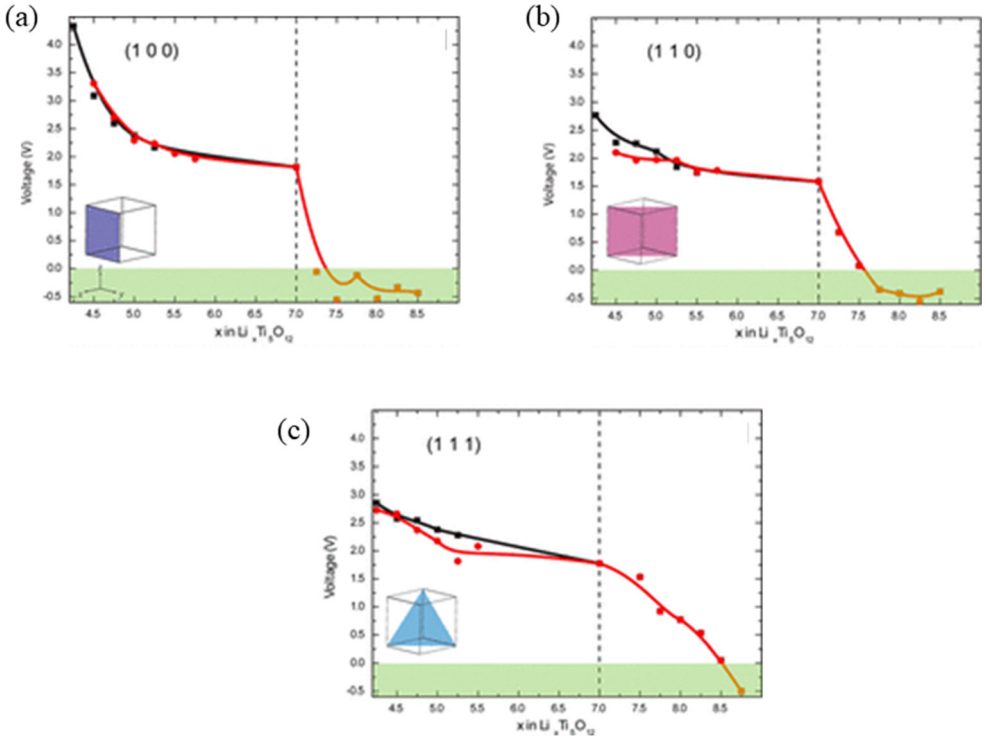

Fig. 5 Voltage profiles of $Li_4Ti_5O_{12}$–$Li_7Ti_5O_{12}$ systems, corresponding to systems whose facets all have (a) (1 0 0), (b) (1 1 0), and (c) (1 1 1) surfaces, respectively. Reprinted with permission from American Chemical Society.[109]

composites, computational work has begun to explore LTO's interfaces with solid-state electrolytes, a critical area for advancing all-solid-state battery technology.[119–121] DFT can resolve the electronic interactions and atomic configurations at solid-state interfaces, allowing predictions of interfacial resistance, the formation of a stable solid electrolyte interface, and chemical stability. Such insights are crucial for guiding the design of solid-state anodes and composites with long-term stability and superior performance.[122] Structural engineering and modification aim to reduce Li^+ diffusion path lengths. It is quantitatively confirmed through GITT and EIS studies that compare the lithium diffusion coefficient along various architectures.[123] Moreover, XPS analysis of near-surface electronic states verifies the surface engineering by confirming the higher concentration of Ti^{3+} near the surface coating.[124]

6.2. Electrochemical correlation

The structural modifications basically affect the surface area, such as in the case of internal structural defects, the band gap narrows about 0.8 to 1.5 eV specifying the improvement in the electronic structure of the material.[125] Other strategies, like composite formation of LTO and carbon, for example, are used for reducing the diffusion distance and improving the conductivity pathway.[126] The surface coatings, most importantly, of Al_2O_3 or amorphous carbon, stabilize the SEI. On an experimental scale, these modifications are confirmed by about 50 to 70% reduction at the interface, referring to high-rate capability and cycling stability.[127] When the maximum number of lithium ions is adsorbed at the LTO structure, the insertion voltage shows a peak at 0.19 eV, which is confirmed by the experimental predictions, where the peak is observed at 0.2 eV.[128] In this way, both kinds of analysis complement each other. The structural modification causes a strain of about 5% in the LTO structure; it can cause a decrease in the insertion voltage plateau in DFT studies, but it does not validate the experimental results because in those results strain percentage can be higher due to factors like grain boundaries and surface effects.[129]

7. Analysis, interplay, and validation

The insight derived from atomistic calculations, while powerful, must be interpreted carefully in the context of experimental reality. A truly impactful review goes beyond summarizing theoretical results; it provides a critical assessment of its accuracy and limitations, thereby shaping future directions. This section synthesizes the findings from previous discussions on doping, defects, and nano-structuring, emphasizing their interconnections and examining how the crucial validation of computational predictions aligns with experimental observations.[130,131]

A primary strength of computational modeling is its ability to uncover the explanations of experimentally observed phenomena. For example, the DFT predictions of the formation of Ti^{3+} polarons in LTO, whether originating from aliovalent doping or intrinsic defects within elements such as Ta^{5+} or Nb^{5+}, have been strongly validated by a suite of characterization techniques.[132–134] EPR and XPS are fluently used to directly quantify and detect the presence of Ti^{3+} species and provide compelling confirmation of theoretical models for improved

electronic conductivity. This correlation provides a strong connection between the macroscopic electronic properties and the charge transfer mechanism.[135,136] The lithium-ion hopping activation energies, which are calculated *via* Nudged Elastic Band (NEB) calculations, are related to the experimental diffusion coefficient, which is measured by several techniques such as Electrochemical Impedance Spectroscopy (EIS).[137,138] In the DFT studies of LTO, performed at high rates, the zero-strain mechanism is predicted, which is further validated by operando XRD lattice parameter measurements (*e.g.* $a = 8.356 \pm 0.001$ Å), which confirms the structural stability.[139] The pure DFT is not able to predict the accurate activation energy of the bulk Li ion diffusion at the low temperature regime, resulting in approximately 0.7 eV, when PFG-NMR and EIS results measure about 0.3 to 0.4 eV.[140] This inconsistency is attributed to the inability of DFT to simulate the necessary long-range defect-mediated pathways at the particle interface. This analysis, based on quantitative data, provides a clear boundary for various recent first-principles methods.[141]

However, discrepancies between theory and experiment are not rare and can create valuable new research questions. For example, standard DFT, being a zero-temperature and static approach, cannot capture the temperature-dependent dynamics and kinetic barriers of a complex synthetic process.[142,143] A dopant predicted to be thermodynamically favorable at a specific site might fail to incorporate effectively in an experiment due to non-equilibrium synthesis routes or kinetic barriers.[33] Moreover, the choice of exchange–correlation functional and, critically, the Hubbard U parameter for localized d-electrons of Ti can lead to variations in the predicted defect formation energies and band gaps.[144,145]

More advanced methods, such as hybrid functionals, can improve accuracy but are computationally expensive and not always suitable for supercell modeling on a large scale. Furthermore, simulations are typically far from idealized, defect-free supercells.[146,147] In contrast, real materials contain grain boundaries, impurities and complex interfaces, which can introduce effects that are difficult for simplified computational models.[148] A notable example is the mismatch between predicted and experimental voltage profiles of LTO. While DFT reliably captures the flat voltage plateau, the exact voltage value is highly sensitive to the choice of U.[149,150] Moreover, the subtle variation observed at the start and end of the plateau is very difficult to reproduce without explicitly considering dynamic structural distortions and defect concentration, factors beyond the scope of DFT calculations.[151] These mismatches are not failures but rather opportunities for an iterative and rigorous feedback loop between experimental synthesis and computational modeling, ultimately accelerating material discoveries.[152]

8. Mutual interplay of design strategies

Achieving a deeper understanding of LTO requires moving beyond the study of isolated phenomena and considering how doping, defects and structural architecture interact.[86] Table 4 compares all the modification techniques discussed for improving LTO as an anode for lithium-ion batteries. This synergistic interplay is a critical frontier in computational research, since the properties of the final material are a result of the combined influence of these factors.[153,154] Fig. 5 shows a visual summary of the modification techniques for LTO, such as doping, defect creation, and structural engineering, and their atomic-level impacts on the structure to enhance its performance activities.

Intrinsic defects, for example, can profoundly affect the stability of doping.[155] The presence of an oxygen vacancy is typically associated with a high formation energy of approximately 1.5 to 3 eV, which can significantly alter the local charge environment, making the nearby site favorable for specific dopant substitution.[156–158] A pentavalent dopant like Nb^{5+} usually generates a Ti^{3+} polaron for charge compensation, might interact with already existing defect clusters in a manner that either suppresses or enhances its electronic effect.[159,160] Computational studies have shown that the dopant incorporation energy landscape is not uniform but is modulated by the local defect environment, highlighting that doping and defects are independent variables.[161–163]

A similar principle governs the interplay between nanostructuring and doping. Both DFT and classical MD calculations show that dopant segregation often occurs when dopants preferentially move to the surface to lower the surface energy and relieve the lattice strain.[164,165] This suggests that a dopant primarily affects the surface diffusion and reactivity.[166] This highlights a crucial link between the efficacy of a doping strategy and the scale of the material (nanoparticles *vs.* bulk) and the efficacy of the doping process.[167] For instance, a dopant

Table 4 Comparison of modification techniques for the LTO anode

No.	Strategy	Mechanism addressed	Key advantage	Limitation	Future aim	Ref.
1	Specific doping (Mg, Al)	Li-ion diffusion barrier	Lower intrinsic energy	Limited conductivity	Use in co-doping	75
2	Co-doping	Kinetic Li and electronic barrier	Improvement in bulk properties	Complicated phase control synthesis	Use in best comprehensive tuning	181
3	Defect engineering	Electronic conductivity (Ti^{3+} defects)	Improved bulk properties	Risk of irreversible capacity loss	Use in electronic tuning	182,183
4	Structural modification (nano-structuring)	Li path length	High carbon-rate improvement at massive loads	Severe SEI growth	Requires surface stabilization	82
5	Surface engineering (N/C coating)	Electronic conductivity	Reduces interfacial impedance	Inactive mass addition to the electrode	Enhancing the conductivity	184

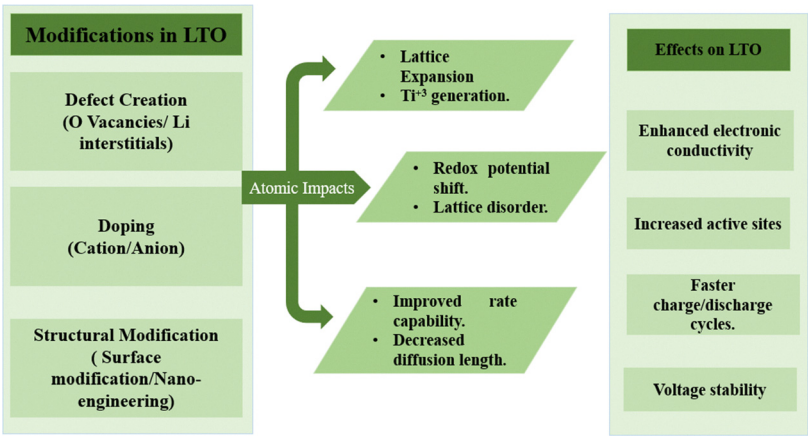

Fig. 6 Summary of engineering strategies for LTO and their atomic-level impacts on the structural properties.

with a large ionic radius, such as Zr^{4+}, may be unsuitable for bulk LTO because of lattice strain but can generate unique surface structures that enhance lithium-ion transfer when segregated to the surface (Fig. 6).[168,169]

Finally, in nano-materials, surface defects play an essential role due to the significant surface-area-to-volume ratio. The faster Li-ion diffusion pathways on a surface, along with a migration barrier of less than 0.2 eV, are notably lower than the typical range of 0.2–0.5 eV.[170,171] These low-barrier pathways are further enhanced or blocked by surface defects.[172] For example, surface lithium vacancies could act as the best hopping sites, whereas antisite defects may act as bottlenecks or traps. Furthermore, the formation energy and thermodynamic stability of defects in a nanoparticle can vary from those in the bulk due to surface energy effects.[173] The intricate relationship between the defect landscape and nano-structuring creates complex and highly non-linear effects on overall performance, necessitating a holistic and integrated computational approach.[174,175] Upon the analytical comparison of all the discussed techniques, different computational methods are applied in each case. MD and KMC (Kinetic Monte Carlo) simulations are used for analyzing the Li-ion diffusion within the structure at the atomic level.[176]

The choice of the Hubbard U parameter is very important as it governs the localized electrons within the d-orbital, which mainly impacts the quantitative results. The electronic properties of transition metal oxide-based electrodes in LIBs are very sensitive to the U parameter. For example, in the case of LTO with U at 0 eV, the value of the bandgap is $\sim$2 eV, but when the value is set at 7 eV, it changes the bandgap value to 3.5 eV, in excellent agreement with the experimental values.[177] In the same way, changing the U_{Co} from 3.3 eV to 5.5 eV in the case of $LiCoO_2$ shifts the bandgap up to 1 eV.[178] In the case of $LiFePO_4$, the standard value of U of 0 eV underestimates the delithiation voltage of the material; the U value of 4.3 eV predicts the voltage of 3.45 eV, which is very near to the experimentally observed value of 3.46 eV.[179] Hence, the U parameter is not just an adjustable parameter, but it has its major role in chemical accuracy against experimental results.[180]

9. Future perspectives and emerging research directions

The preceding sections have highlighted the profound impact of computational modeling on advancing and understanding LTO at the atomic scale. Yet, significant challenges persist, demanding a shift towards more integrated, dynamic, and advanced computational approaches. The future of LTO research lies in moving beyond static, high-throughput approaches that can bridge the gap between real-world and idealized models, single-variable investigations towards multi-scale and real-world electrochemical performance, enabling the rational design of future LTO anodes.[185–187]

A key limitation of conventional DFT is its emphasis on static pathways and ground-state properties.[188] While excellent for migration barriers and formation energies, it falls short in describing the dynamic processes that are critical for governing battery performance.[189] The next frontier for computational research in LTO is to portray complex phenomena such as full charge–discharge kinetics and the formation of a solid–electrolyte interphase (SEI) under realistic operation conditions.[190] The SEI is a notoriously complex, reactive layer whose growth and nucleation are governed by dynamic reaction on the surface of LTO, processes beyond the scope of conventional DFT.[191,192] Similarly, understanding capacity fading and stability under repeated cycling requires a computational framework capable of simulating atomic motions over finite temperatures and an extended time scale.[193]

These techniques are useful in overcoming the challenges faced by modified LTO; still, some key areas require further improvements. The major bottleneck lies in having control over the evolution of SEIs; although LTO operates at a typical reduction potential of electrolyte, low temperature, and accelerated cycling can induce heterogeneous SEI formation. This causes impedance growth and capacity fading as well.[194] The future DFT studies are supposed to move beyond static surface models to incorporate the role of localized defects and electrolyte decomposition kinetics, providing a strong and direct link to experimental cell aging. Secondly, the effectiveness of the

bulk is compromised by the dopant segregation. Atomic-resolution STEM-EEL experimental analysis consistently reveals that p-block dopants and transition metals preferentially migrate to the particle surface or towards grain boundaries, forming secondary insulating and resistive phases, effectively counteracting the improvements in electronic conductivity.[195] A very focused experimental work is required to match the results of the DFT studies performed on all the techniques of enhancing the performance of LTO. Moreover, significant discrepancies remain between experimental and DFT-based profiles for the LTO/$Li_7Ti_5O_{12}$ phase transition. The standard GGA+U functional normally overmeasures the characteristic ~1.55 V plateau by 0.1–0.2 V, due to insufficient treatment of weak interaction within the spinel lattice and redox processes.[196] The development of more advanced functionals such as Dynamic Mean Field Theory (DMFT) and Hybrid Density Functionals (HSE06) is important to achieve the sub-0.05 accuracy needed to make new materials with modified designs and fill the gap between theoretical and experimental works.[197]

To overcome these simulations, two emerging computational directions are set to reshape the field. The first is Machine Learning (ML) potentials, poised to enable high-throughput screening of vast chemical design spaces.[198] This strategy eliminates the need for the time-consuming process of individual DFT calculations for each defect configuration or dopant. For instance, ML-based calculations are approximately 10^6 times faster than traditional DFT, enabling the rapid screening of potential dopants to identify suitable candidates for further experimental investigation.[185,199,200] Likewise, AIMD offers a powerful framework to study the dynamic evolution of LTO systems. In contrast to static NEB calculations, which provide a single minimum-energy migration pathway, AIMD can capture complex, Li-ion hopping mechanisms and describe ion transport under thermal agitation. It is also an ideal tool for investigating the initial stages of SEI development at the electrode–electrolyte interface, offering critical insights into structural changes and chemical reactions that lead to the formation of the protective layer.[152,201,202]

DFT, as the base of AIMD, exhibits the highest accuracy as a quantum mechanical method. It is, though limited by the computational cost ($O(N^3)$ or worse, here N is the number of atoms), which tries to reduce the scalability to short simulations and small systems.[203] The machine learning potentials offer near DFT accuracy and bridge this gap at a reduced computational cost ($O(N)$). This results in better scalability and a larger timescale.[204] The AIMD simulations therefore, provide finite-temperature information with accuracy and suffer from the same computational scaling, so they are considered as the least scalable and most expensive among the three of the larger systems.[205] Recent studies have shown that the cubic scaling cost of DFT restricts the simulations to a smaller cell size and time scale, which is considered insufficient for ion transport at a long range. On the other hand, the ML trained on the principles of DFT data can attain the *ab initio* accuracy within the cost of MD at approximately 10^{-3} of the speed of DFT.[206] This is a high-scale efficiency as it allows the AIMD-level accuracy over the extended timescale of nano-seconds and large-scale simulations of approximately 10^3 atoms.[207] It enables the investigation of various crucial phenomena like the temperature-dependent lithium diffusion pathway, which governs the cyclability and stability of the electrode material.[208]

The true value of machine learning approaches such as the Gaussian Approximation Potential (GAP) resides in their exceptional capability to bridge the computational gap. Specifically, in the case of LTO anode materials for lithium-ion batteries, this has been demonstrated by ML interatomic potentials to reproduce the DFT-level energy barriers for the migration of Li-ions in $LiFePO_4$.[209] Mainly, these potentials allow the larger simulations to happen in the nanoscale time range for the supercells containing thousands of atoms, such as bulk LTO containing nano-voids.[210] The diffusion studies and the traditional AIMD simulations, which are difficult to attain a specific magnitude, can easily be reached. Such computational gain is very important in accurately capturing the long-range defect-mediated diffusion and grain boundary effects in any kind of materials, including lithium-ion battery materials.[211]

The ultimate goal of these advanced methodologies is to establish a stronger feedback loop between computational modelers and experimentalists, which is crucial for evolving the development of new LTO anode strategies. Traditionally, these two fields have progressed in silos. In the future, this relationship will become a reciprocal exchange.[212,213] Experimentalists will provide the real-world data about various failure modes of the material related to strategies such as defect concentration, structural design, or doping. The computational community can use these data to address issues such as why a specific dopant showed a different rate performance than expected.[214,215] In turn, dynamic simulations and high-throughput screening can be used to propose valid predictions for complex co-doping strategies and new defect-engineered structures. This iterative cycle is crucial for accelerating the rational design of next-generation anode materials and moving beyond the serendipitous discovery that has long dominated battery research.[216–218]

10. Summary

This comprehensive review has demonstrated that computational modeling has been instrumental in advancing the basic understanding of $Li_4Ti_5O_{12}$ and designing strategies for its enhanced performance. First-principles calculations have demonstrated the atomic-scale origin of LTO's electrochemical behavior, revealing how targeted doping and defect engineering address its electronic conductivity-related issues, while the principles have provided pathways to overcome its slow ionic kinetics. The key finding from this body of work is the non-linear interplay between these strategies. A comprehensive understanding of the influence of these strategies upon each other is essential for the design of a high-performance LTO anode.

Despite significant progress, major challenges such as long-term capacity fading, unlocking higher theoretical capacities, and understanding SEI evolution still require a more integrated and dynamic approach. Overcoming these obstacles requires moving beyond the static limitations of conventional methods. This review highlights that the ultimate objective of these strategies is to enhance the performance of LTO anodes. By introducing intrinsic defects, we can enhance charge transport within the bulk material, enabling faster charging and higher power density. Theoretical insights into antisite defects and lithium vacancies have paved the way for controlled synthesis methods to enhance lithium-ion mobility. Charge carriers are created due to doping in the structure; these charge carriers play a vital role in enhancing the electronic conductivity. Designing a material with better diffusion rates and structural stability results in higher C-rates and enhanced material performance. One of the major points in understanding strategic techniques, such as co-doping, for enhanced electrochemical performance is to understand the screening methods that overcome the kinetic limitations and play a vital role in stabilizing the reactive surfaces. Designing complex composites of conductive materials with LTO also enhances material performance to a greater extent. Along with all these techniques for performance enhancement, understanding of factors, such as interactions between the solid electrolyte and LTO, is important for predicting interfacial resistance and enhancing material stability. Most importantly, the ultimate goal is to pick the most accurate strategy for incorporation in the material, according to the needs of the time, and study its effects accurately through appropriate DFT simulations.

Conflicts of interest

There are no conflicts to declare.

Data availability

No primary research results, software or code have been included and no new data were generated or analysed as part of this review.

References

1 F. Khan, Design and optimization of lithium-ion battery as an efficient energy storage device for electric vehicles, 2023, CQUniversity.
2 S. El Afia, *et al.*, Rechargeable Li-Ion Batteries, Nanocomposite Materials and Applications, *Batteries*, 2024, **10**(12), 413.
3 M. D. Ahmed and K. M. Maraz, Revolutionizing energy storage: Overcoming challenges and unleashing the potential of next generation Lithium-ion battery technology, *Mater. Eng. Res.*, 2023, **5**(1), 265–278.
4 M. Wakihara, Recent developments in lithium ion batteries, *Mater. Sci. Eng., R*, 2001, **33**(4), 109–134.
5 N. Nandihalli, A review of nanocarbon-based anode materials for lithium-ion batteries, *Crystals*, 2024, **14**(9), 800.
6 J. Ye, *et al.*, Controlling of the ratio of submicron particles and size effects in SiO anode for Li-ion batteries, *Sustainable Mater. Technol.*, 2024, **41**, e01109.
7 J. H. Choi and P. Oh, Analysis of Electrochemical Properties of Sulfide All-Solid-State Lithium Ion Battery Anode Material Using Amorphous Carbon-Removed Graphite, *Appl. Chem. Eng.*, 2022, **33**(1), 58–63.
8 B. Gürünlü, Ç. Taşdelen-Yücedağ and M. Bayramoğlu, One pot synthesis of graphene through microwave assisted liquid exfoliation of graphite in different solvents, *Molecules*, 2022, **27**(15), 5027.
9 J. Asenbauer, *et al.*, The success story of graphite as a lithium-ion anode material–fundamentals, remaining challenges, and recent developments including silicon (oxide) composites, *Sustainable Energy Fuels*, 2020, **4**(11), 5387–5416.
10 H. Zhang, *et al.*, Graphite as anode materials: Fundamental mechanism, recent progress and advances, *Energy Storage Mater.*, 2021, **36**, 147–170.
11 R. Wang, *et al.*, Highly fluorinated co-solvent enabling ether electrolyte for high-voltage lithium-ion batteries with graphite anode, *Energy Mater.*, 2023, **3**(5), 300040.
12 F. Linsenmann, *et al.* Formation of the solid electrolyte interphase on the graphite anode in lithium-ion batteries–an operando neutron depth profiling study. in Electrochemical Society Meeting Abstracts 236, 2019, The Electrochemical Society, Inc.
13 R. Yazami and Y. F. Reynier, Mechanism of self-discharge in graphite–lithium anode, *Electrochim. Acta*, 2002, **47**(8), 1217–1223.
14 C. Sandhya, B. John and C. Gouri, Lithium titanate as anode material for lithium-ion cells: a review, *Ionics*, 2014, **20**(5), 601–620.
15 G. N. Zhu, *et al.*, Binary Li4Ti5O12-Li2Ti3O7 nanocomposite as an anode material for Li-Ion batteries, *Adv. Funct. Mater.*, 2013, **23**(5), 640–647.
16 Q. Huang, Z. Yang and J. Mao, Mechanisms of the decrease in low-temperature electrochemical performance of Li4Ti5O12-based anode materials, *Sci. Rep.*, 2017, **7**(1), 15292.
17 L. Mo and H. Zheng, Solid coated Li4Ti5O12 (LTO) using polyaniline (PANI) as anode materials for improving thermal safety for lithium ion battery, *Energy Rep.*, 2020, **6**, 2913–2918.
18 H. Jin, *et al.*, Novel lithium titanate for high power applications, *ECS Trans.*, 2014, **58**(48), 63.
19 B. Ziebarth, *et al.*, Lithium diffusion in the spinel phase $Li_4Ti_5O_{12}$ and in the rocksalt phase $Li_7Ti_5O_{12}$ of lithium titanate from first principles, *Phys. Rev. B:Condens. Matter Mater. Phys.*, 2014, **89**(17), 174301.
20 E. Zhao, *et al.*, Lithium titanate confined in carbon nanopores for asymmetric supercapacitors, *ACS Nano*, 2016, **10**(4), 3977–3984.
21 B.-S. Lee, A review of recent advancements in electrospun anode materials to improve rechargeable lithium battery performance, *Polymers*, 2020, **12**(9), 2035.

22 J. P. Zheng, The limitations of energy density of battery/double-layer capacitor asymmetric cells, *J. Electrochem. Soc.*, 2003, **150**(4), A484.
23 Y. Huang, *et al.*, Li-ion battery material under high pressure: amorphization and enhanced conductivity of Li4Ti5O12, *Natl. Sci. Rev.*, 2019, **6**(2), 239–246.
24 W. Borghols, *et al.*, The electronic structure and ionic diffusion of nanoscale $LiTiO_2$ anatase, *Phys. Chem. Chem. Phys.*, 2009, **11**(27), 5742–5748.
25 N. Z. K. Razali, *et al.*, DFT, Fukui indices, and molecular dynamic simulation studies on corrosion inhibition characteristics: a review, *Chem. Pap.*, 2024, **78**(2), 715–731.
26 E. O. Gomes, *et al.*, Computational procedure to an accurate DFT simulation to solid state systems, *Comput. Mater. Sci.*, 2019, **170**, 109176.
27 R. El Haouti, *et al.*, Cationic dyes adsorption by Na-Montmorillonite Nano Clay: Experimental study combined with a theoretical investigation using DFT-based descriptors and molecular dynamics simulations, *J. Mol. Liq.*, 2019, **290**, 111139.
28 H. Singh, *et al.*, Identification of dopant site and its effect on electrochemical activity in Mn-doped lithium titanate, *Phys. Rev. Mater.*, 2018, **2**(12), 125403.
29 H. S. Bhatti, *et al.*, Correlation of Electrochemical Characteristics with Structural, Optical, and Electrical Properties in Tungsten-Doped Li4Ti5O12 Anodes, *J. Phys. Chem. C*, 2023, **127**(16), 7580–7594.
30 A. Fitriah, *et al.*, The Density Functional Theory Study of Li-ion diffusion in Na-doped Li4Ti5O12 as lithium-ion battery anode, *Spektra: J. Fis. Apl.*, 2022, **7**(3), 151–158.
31 K. K. Surthi, M. Thak and K. K. Kar, Charge–discharge mechanism, lithium-ion diffusion in Al, Ca, and Cu doped lithium metatitanate based anodes for Li-ion batteries: first principles study, *J. Mater. Chem. A*, 2024, **12**(20), 12098–12111.
32 J. Gong, *et al.*, Carbon-coated Li4Ti5O12 particle anchored on reduced graphene oxide for Li-ion batteries, *J. Electroanal. Chem.*, 2024, **952**, 117932.
33 C. H. Lee and S. U. Lee, p-and n-type Doping Effects on the Electrical and Ionic Conductivities of Li4Ti5O12 Anode Materials, *J. Phys. Chem. C*, 2018, **122**(27), 15155–15162.
34 A. Jain, Y. Shin and K. A. Persson, Computational predictions of energy materials using density functional theory, *Nat. Rev. Mater.*, 2016, **1**(1), 1–13.
35 J. Shen, *et al.*, Surface/interface structure and chemistry of lithium–sulfur batteries: from density functional theory calculations' perspective, *Adv. Energy Sustainability Res.*, 2021, **2**(6), 2100007.
36 M. D. Johannes, C. T. Love and K. Swider-Lyons, Calculations in li-ion battery materials, *Springer Handbook of Electrochemical Energy*, Springer, 2016, pp. 313–328.
37 H. Euchner and A. Groß, Atomistic modeling of Li-and post-Li-ion batteries, *Phys. Rev. Mater.*, 2022, **6**(4), 040302.
38 S. C. Liebscher, *et al.*, Extension of the LDA-1/2 method to the material class of bismuth containing III–V semiconductors, *AIP Adv.*, 2020, **10**(11), 115003.
39 M. Lewin, E. H. Lieb and R. Seiringer, The local density approximation in density functional theory, *Pure Appl. Anal.*, 2019, **2**(1), 35–73.
40 A. Urban, D.-H. Seo and G. Ceder, Computational understanding of Li-ion batteries, *npj Comput. Mater.*, 2016, **2**(1), 1–13.
41 Q. Sun and Y. Yin, Theoretical exploration of band gap error dependency on band gap size in density functional theory Calculations: CdTe and GeTe as representative cases of two band structure semiconductor types, *Comput. Mater. Sci.*, 2024, **239**, 112956.
42 G. Cai, *et al.*, Predicting structure-dependent Hubbard U parameters via machine learning, *Mater. Futures*, 2024, **3**(2), 025601.
43 Y. Zhang, *et al.*, Extended Lagrangian Born-Oppenheimer Molecular Dynamics with DFT+U, *arXiv*, 2023, preprint, arXiv:2303.03655, DOI: 10.48550/arxiv.2303.03655.
44 N. J. Mosey and E. A. Carter, Ab initio evaluation of Coulomb and exchange parameters for DFT+U calculations, *Phys. Rev. B:Condens. Matter Mater. Phys.*, 2007, **76**(15), 155123.
45 H. Chen, *et al.*, Diffusion-Equation-Based Electrical Modeling for High-Power Lithium Titanium Oxide Batteries, *Batteries*, 2024, **10**(7), 238.
46 T. Cleary, *et al.*, Electrical and thermal modeling of a large-format lithium titanate oxide battery system, 2015, Mineta National Transit Research Consortium.
47 F. Ferrante, *et al.*, H2 transformations on graphene supported palladium cluster: Dft-md simulations and neb calculations, *Catalysts*, 2020, **10**(11), 1306.
48 C. Takashima and H. Nakai, Range Separation Method for Density Functional Theory Based on Two-Electron Infinite-Order Two-Component Hamiltonian, *J. Chem. Theory Comput.*, 2024, **20**(2), 738–751.
49 V. V. Shunaev, *et al.*, Two-dimensional films based on graphene/Li4Ti5O12 and carbon nanotube/Li4Ti5O12 nanocomposites as a prospective material for lithium-ion batteries: insight from Ab initio modeling, *Materials*, 2023, **16**(8), 3270.
50 Q. Cui, *et al.*, Recent advances in designing high-capacity anode nanomaterials for Li-ion batteries and their atomic-scale storage mechanism studies, *Adv. Sci.*, 2018, **5**(7), 1700902.
51 Y.-H. Zhang, *et al.*, Ultrahigh lithiation dynamics of Li4Ti5O12 as an anode material with open diffusion channels induced by chemical presodiation, *Rare Met.*, 2023, **42**(2), 471–483.
52 S. Lkhagvajav, *et al.*, Structural and electronic properties of the spinel $Li_4Ti_5O_{12}$, *Mong. J. Chem.*, 2019, **20**(46), 7–12.
53 M. Kick, *et al.*, Mobile Small Polarons Explain Conductivity in Lithium Titanium Oxide Battery Electrodes, *arXiv*, 2020, preprint, arXiv:2001.00263, DOI: 10.48550/arxiv.2001.00263.
54 Y.-T. Chan, *et al.*, The origin of enhanced conductivity and structure change in defective Li4Ti5O12: a study combining theoretical and experimental perspectives, *J. Mater. Chem. A*, 2025, **13**, 32149–32158.
55 L. Noerochim, *et al.*, Direct double coating of carbon and nitrogen on fluoride-doped Li4Ti5O12 as an anode for lithium-ion batteries, *Batteries*, 2022, **8**(1), 5.

56 K. Doll, N. Harrison and V. Saunders, A density functional study of lithium bulk and surfaces, *J. Phys.: Condens. Matter*, 1999, **11**(26), 5007.
57 I. I. Idowu, *et al.*, Investigating the Influence of Exchange–correlation Effects and the Hubbard Term on the Electronic Bands of Defected Cu2O: A Dft Study. 2024.
58 J. Hermet, C. Adamo and P. Cortona, Towards a greater accuracy in dft calculations: From gga to hybrid functionals, *Quantum Simulations of Materials and Biological Systems*, Springer, 2012, pp. 3–15.
59 R. R. Marek, Predicting Supramolecular Interactions and Properties of Systems by Methods of Computational Chemistry.
60 C. Dong, *et al.*, Recent progress and perspectives of defective oxide anode materials for advanced lithium ion battery, *EnergyChem*, 2020, **2**(6), 100045.
61 Y.-X. Yu, Can all nitrogen-doped defects improve the performance of graphene anode materials for lithium-ion batteries?, *Phys. Chem. Chem. Phys.*, 2013, **15**(39), 16819–16827.
62 Z. Su, *et al.*, Quenching-induced defects liberate the latent reversible capacity of lithium titanate anode, *Adv. Mater.*, 2023, **35**(5), 2208573.
63 Y.-C. Pak, *et al.*, Defect formation and ambivalent effects on electrochemical performance in layered sodium titanate $Na_2Ti_3O_7$, *Phys. Chem. Chem. Phys.*, 2023, **25**(4), 3420–3431.
64 L. Zhang, *et al.*, Atomic defect mediated Li-ion diffusion in a lithium lanthanum titanate solid-state electrolyte, *ACS Nano*, 2022, **16**(4), 6898–6905.
65 D. V. Pelegov, *et al.*, Defects in $Li_4Ti_5O_{12}$ induced by carbon deposition: An analysis of unidentified bands in Raman spectra, *Phys. Chem. Chem. Phys.*, 2019, **21**(37), 20757–20763.
66 H. Duan, *et al.*, Tailoring native defects and zinc impurities in Li4Ti5O12: insights from first-principles study. The, *J. Phys. Chem. C*, 2015, **119**(9), 5238–5245.
67 W. Choi, *et al.*, Defective lithium titanate oxide with stable cycling over a wide voltage window, *Appl. Surf. Sci.*, 2023, **614**, 156134.
68 J. Fang, *et al.*, Break the capacity limit of Li4Ti5O12 anodes through oxygen vacancy engineering, *Chin. J. Struct. Chem.*, 2025, **44**(2), 100504.
69 Y. Bai, *et al.*, Oxygen vacancy content drives self-reduction and anti-thermal quenching, *J. Mater. Chem. C*, 2022, **10**(11), 4317–4326.
70 J. Dawson, *et al.*, First-principles study of intrinsic point defects in hexagonal barium titanate, *J. Appl. Phys.*, 2012, **111**(9), 094108.
71 P. Ágoston, *et al.*, Geometry, electronic structure and thermodynamic stability of intrinsic point defects inindium oxide, *J. Phys.: Condens. Matter*, 2009, **21**(45), 455801.
72 K. Suzuki, Y. Ito and H. Miura, Influence of Intrinsic Defects and Strain on Electronic Reliability of Gate Oxide films, *MRS Online Proc. Libr.*, 2006, **917**, 0917-E05-28.
73 A. Y. Golovacheva and P. D'yachkov, Effect of intrinsic defects on the electronic structure of BN nanotubes; Vliyanie sobstvennykh defektov na ehlektronnoe stroenie BN-nanotrubok. Pis' ma v Zhurnal Ehksperimental'noj i Teoreticheskoj Fiziki, 2005. **82**.
74 Y. Zhang, *et al.*, Defect engineering on electrode materials for rechargeable batteries, *Adv. Mater.*, 2020, **32**(7), 1905923.
75 H. Cho, *et al.*, Impact of Mg-doping site control in the performance of Li4Ti5O12 Li-ion battery anode: first-principles predictions and experimental verifications, *J. Phys. Chem. C*, 2017, **121**(28), 14994–15001.
76 S. Yeo, M. R. Raj and G. Lee, Oxygen vacancy-modulated zeolitic Li4Ti5O12 microsphere anode for superior lithium-ion battery, *Electrochim. Acta*, 2023, **441**, 141809.
77 F. Zhang, *et al.*, Enhanced stability and the lithium storage mechanism of oxygen vacancy-induced heterogeneous $Li_4Ti_5O_{12}/TiO_2$ (B) anolytes, *J. Mater. Chem. A*, 2024, **12**(29), 18393–18403.
78 H. Lim, M. A. Abbas and J. H. Bang, Memory effect in lithium titanate driven by interfacial oxygen vacancies, *ACS Energy Lett.*, 2022, **7**(3), 1086–1091.
79 T. Meng, *et al.*, Engineering of oxygen vacancy and electric-field effect by encapsulating lithium titanate in reduced graphene oxide for superior lithium ion storage, *Small Methods*, 2019, **3**(10), 1900185.
80 D. Young, *et al.*, Electronic conductivity in the Li4/3Ti5/3O4–Li7/3Ti5/3O4 system and variation with state-of-charge as a Li battery anode, *Adv. Energy Mater.*, 2013, **3**(9), 1125–1129.
81 L. Yan, *et al.*, High-pressure induction and quantitative regulation of oxygen vacancy defects in lithium titanate, *Adv. Funct. Mater.*, 2023, **33**(34), 2301886.
82 J. Cervantes, *et al.*, DFT Electronic Properties and Synthesis Thermodynamics of Li x La1− x TiO3 Electrolytes for Li-Ion Batteries, *J. Electrochem. Soc.*, 2021, **168**(8), 080516.
83 M. Shen, *et al.*, Theoretical prediction and experimentally realizing cathodic doping of sulfur in Li4Ti5O12 for superior lithium storage performance, *ACS Appl. Energy Mater.*, 2021, **4**(6), 5995–6004.
84 L. Wang, *et al.*, Structural and electrochemical characteristics of Ca-doped ''flower-like'' Li4Ti5O12 motifs as high-rate anode materials for lithium-ion batteries, *Chem. Mater.*, 2018, **30**(3), 671–684.
85 Y. Tanaka, *et al.*, First-principles analysis on role of spinel (111) phase boundaries in $Li_{4+3x}Ti_5O_{12}$ Li-ion battery anodes, *Phys. Chem. Chem. Phys.*, 2016, **18**(33), 23383–23388.
86 P.-C. Tsai, *et al.*, Ab initio phase stability and electronic conductivity of the doped-Li4Ti5O12 anode for Li-ion batteries, *Acta Mater.*, 2019, **175**, 196–205.
87 H.-m Kim, *et al.*, Mixed anion effects on structural and electrochemical characteristics of $Li_4Ti_5O_{12}$ for high-rate and durable anode materials, *J. Mater. Chem. A*, 2024, **12**(12), 7107–7121.
88 K. Tada, M. Kitta and S. Tanaka, Properties of spinel-type Ti–Li–M composite oxides (M= Li, Na, Cu, and Ag) predicted by density functional theory, *Phys. Chem. Chem. Phys.*, 2022, **24**(45), 28055–28068.
89 D. Shao, *et al.*, How the sodium cations in anode affect the performance of a Lithium-ion battery, *Batteries*, 2022, **8**(8), 78.
90 K. L. Salvatore, *et al.*, Solution-Based, Anion-Doping of Li4Ti5O12 Nanoflowers for Lithium-Ion Battery Applications, *Chem. – Eur. J.*, 2020, **26**(42), 9389–9402.

91 M. M. Asadov, *et al.*, Modeling of Structural Properties of Zr (Nb)-Doped c-LTO–Zr (Nb) Materials With Spinel Structure for Li-Ion Batteries, *WSEAS Trans. Electron.*, 2024, **15**, 166–183.
92 Z. Wang, *et al.*, A First-Principles Study of Anion Doping in LiFePO4 Cathode Materials for Li-Ion Batteries, *Chem. Phys. Chem.*, 2024, **25**(3), e202300756.
93 J. Wang, *et al.* Computational Studies of the Effect of Nitrogen Dopants and Oxygen Vacancies on Li+ Conduction in Lithium Lanthanum Titanate Electrolytes. in Electrochemical Society Meeting Abstracts 243. 2023. The Electrochemical Society, Inc.
94 F. Kong, *et al.*, Conflicting roles of anion doping on the electrochemical performance of Li-ion battery cathode materials, *Chem. Mater.*, 2016, **28**(19), 6942–6952.
95 W. Cheng, *et al.*, In situ topotactic preparation of porous plate-like Li2ZnTi3O8 as the lithium-ion batteries anode for enhancing electrochemical reaction kinetics and Li+ storage, *Electrochim. Acta*, 2023, **440**, 141758.
96 C. Li, Q. Huang and J. Mao, Improve the low-temperature electrochemical performance of Li4Ti5O12 anode materials by ion doping, *J. Mater. Sci.: Mater. Electron.*, 2020, **31**(23), 21444–21454.
97 Y. Li, H. Gao and W. Yang, Enhancements of the structures and electrochemical performances of Li4Ti5O12 electrodes by doping with non-metallic elements, *Electrochim. Acta*, 2022, **409**, 139993.
98 A. Lakshmi-Narayana, *et al.*, Enhanced electrochemical performance of rare-earth metal-ion-doped nanocrystalline Li4Ti5O12 electrodes in high-power Li-ion batteries, *ACS Appl. Mater. Interfaces*, 2023, **15**(17), 20925–20945.
99 I. Batsukh, *et al.*, Investigation of structural, optical, and electrochemical properties of niobium-doped Li4Ti5O12 for high-performance aqueous capacitor electrode, *Ceram. Int.*, 2023, **49**(16), 26313–26321.
100 S. Priyono, B. Prihandoko and A. H. Yuwono, High electrochemical performance of Al-doped Li4Ti5O12 (LTO) with prepared via sol–gel route at low pH as anode for lithium ion battery, *AIP Conf. Proc.*, 2021, 040013.
101 P. Jakes, *et al.*, Mixed ionic-electronic conducting Li4Ti5O12 as anode material for lithium ion batteries with enhanced rate capability-impact of oxygen non-stoichiometry and aliovalent Mg2 + -doping studied by electron paramagnetic resonance, *Z. Phys. Chem.*, 2015, **229**(9), 1439.
102 L. Hou, *et al.*, Zr-doped Li4Ti5O12 anode materials with high specific capacity for lithium-ion batteries, *J. Alloys Compd.*, 2019, **774**, 38–45.
103 R. Sukumar, P. Iyngaran and N. Kuganathan, Structural and Defect Properties of LiTi2 (PO4)3, *Biointerface Res. Appl. Chem.*, 2021, **11**, 13268–13275.
104 A. Xia, *et al.*, Influence of fluorine doping on the structure and electrochemical performance of δ-MnO2 for supercapacitors, *Ceram. Int.*, 2024, **50**(8), 13061–13069.
105 G. Xu, *et al.*, Highly-crystalline ultrathin gadolinium doped and carbon-coated Li4Ti5O12 nanosheets for enhanced lithium storage, *J. Power Sources*, 2015, **295**, 305–313.
106 S. Ullah, *et al.*, Band-gap tuning of graphene by Be doping and Be, B co-doping: a DFT study, *RSC Adv.*, 2015, **5**(69), 55762–55773.
107 M. Kick, C. Scheurer and H. Oberhofer, Formation and stability of small polarons at the lithium-terminated $Li_4Ti_5O_{12}$ (LTO)(111) surface, *J. Chem. Phys.*, 2020, **153**(14), 144701.
108 J. Su, *et al.*, Improving the heterointerface in hybrid organic–inorganic perovskite solar cells by surface engineering: Insights from periodic hybrid density functional theory calculations, *J. Comput. Chem.*, 2020, **41**(19), 1740–1747.
109 S. Ganapathy and M. Wagemaker, Nanosize storage properties in spinel Li4Ti5O12 explained by anisotropic surface lithium insertion, *ACS Nano*, 2012, **6**(10), 8702–8712.
110 Y. Ren, *et al.*, Three-Phase Transition of Spinel Li4Ti5O12 with a Dense Single-Particle Microelectrode in Li-Ion Batteries, *Energy Fuels*, 2024, **38**(17), 16976–16983.
111 D. S. Kim, *et al.*, Surface engineering of graphite anode material with black TiO2-x for fast chargeable lithium ion battery, *Electrochim. Acta*, 2017, **258**, 336–342.
112 S. Choi, Study on Nano-Engineering of High-Capacity Anode Materials for High-Power Energy Storage System. 2015, Ulsan National Institute of Science and Technology (UNIST).
113 C. Lin, *et al.*, Advanced electrochemical performance of Li4Ti5O12-based materials for lithium-ion battery: synergistic effect of doping and compositing, *J. Power Sources*, 2014, **248**, 1034–1041.
114 M. Wang, *et al.*, Synthesis of Highly Stable LTO/rGO/SnO2 Nanocomposite via In Situ Electrostatic Self-Assembly for High-performance Lithium-Ion Batteries, *Adv. Funct. Mater.*, 2023, **33**(30), 2213902.
115 L. De Souza, *et al.*, A DFT investigation of lithium adsorption on graphenes as a potential anode material in lithium-ion batteries, *J. Mol. Graphics Modell.*, 2021, **108**, 107998.
116 J. Gomez Quispe, *et al.*, Tpdh-graphene as a new anodic material for lithium ion battery: Dft-based investigations, *ACS Omega*, 2024, **9**(37), 39195–39201.
117 S. Shanmugam, S. Nachimuthu and V. Subramaniam, Enhanced Li+ ion adsorption on pristine and defected graphene via organic radical interaction–A DFT study, *Phys. B*, 2021, **611**, 412700.
118 M. H. Mamme, *et al.* Insights on Solid–electrolyte/electrode interfaces of All-solid-state Batteries: Multiscale Framework. in Electrochemical Society Meeting Abstracts 243. 2023. The Electrochemical Society, Inc.
119 R. Iwasaki, *et al.*, Density Functional Theory Studies on Li Metal Electrode/Garnet-Type Li7La3Zr2O12 Solid Electrolyte Interfaces for Application in All-Solid-State Batteries, *Phys. Status Solidi B*, 2022, **259**(9), 2100546.
120 T.-Y. Ahn, *et al.*, Orientational Relationship Between the Solid-Electrolyte Interphase and $Li_4Ti_5O_{12}$ Electrode in Hybrid Aqueous Electrolytes, *J. Electrochem. Sci. Technol.*, 2024, **15**(4), 476–483.
121 S. Lee, *et al.*, Unveiling crystal orientation-dependent interface property in composite cathodes for solid-state

batteries by in situ microscopic probe, *Nat. Commun.*, 2024, **15**(1), 7947.
122 A. Hasani, *et al.*, Localized Phase and Elemental Mapping in Solid-State Lithium Battery LTO Anode Thin-Film Produced by a Novel Suspension Plasma Spray Approach, *J. Therm. Spray Technol.*, 2025, 1–9.
123 B. Gangaja, S. Nair and D. Santhanagopalan, Surface-engineered Li4Ti5O12 nanoparticles by TiO2 coating for superior rate capability and electrochemical stability at elevated temperature, *Appl. Surf. Sci.*, 2019, **480**, 817–821.
124 Y. Huang, *et al.*, Surface coating with Li-Ti-O to improve the electrochemical performance of Ni-rich cathode material, *Appl. Surf. Sci.*, 2019, **489**, 913–921.
125 W. Li, *et al.*, Structural and electrochemical characteristics of SiO2 modified Li4Ti5O12 as anode for lithium-ion batteries, *J. Alloys Compd.*, 2015, **637**, 476–482.
126 Z. Chen, *et al.*, Li4Ti5O12 anode: structural design from material to electrode and the construction of energy storage devices, *Chem. Rec.*, 2018, **18**(3), 350–380.
127 C. Chen, R. Agrawal and C. Wang, High performance Li4Ti5O12/Si composite anodes for Li-ion batteries, *Nanomaterials*, 2015, **5**(3), 1469–1480.
128 S. Subash, *et al.*, Insight into Engineering the LMNO/LLTO/LTO Thin-Film Solid-State Micro Batteries: Structural Understandings and Electrochemical Evaluation, *Electrochim. Acta*, 2025, 147113.
129 F. de Haan-de Wilde and M. Janssen. An Update of the Assessment Methodology for Civil Ageing Management for LTO/CSO Based on International Standards and Engineering Judgement. in Pressure Vessels and Piping Conference. 2021. American Society of Mechanical Engineers.
130 W. J. Weber, *et al.*, Experimental and computational studies of ion-solid interactions in silicon carbide. MRS Online Proceedings Library (OPL), 2003. 792, R5. 1.
131 K. Hoang and M. Johannes, Defect physics in complex energy materials, *J. Phys.:Condens. Matter*, 2018, **30**(29), 293001.
132 V. Kumaravel, *et al.*, Unravelling the impact of Ta doping on the electronic and structural properties of titania: A combined theoretical and experimental approach, *J. Phys. Chem. C*, 2022, **126**(4), 2285–2297.
133 M. S. Marshall, *et al.*, Atomic and electronic surface structures of dopants in oxides: STM and XPS of Nb-and La-doped $SrTiO_3$(001), *Phys. Rev. B:Condens. Matter Mater. Phys.*, 2011, **83**(3), 035410.
134 C. Di Valentin, *et al.*, Characterization of paramagnetic species in N-doped TiO2 powders by EPR spectroscopy and DFT calculations, *J. Phys. Chem. B*, 2005, **109**(23), 11414–11419.
135 M. Reticcioli, U. Diebold and C. Franchini, Modeling polarons in density functional theory: lessons learned from TiO2, *J. Phys.: Condens. Matter*, 2022, **34**(20), 204006.
136 W.-D. Yang, X-ray photoelectron spectroscopy and electrical properties studies of Nb-doped strontium titanate ceramics prepared from titanyl acylate precursors, *J. Electron. Mater.*, 1999, **28**(8), 986–995.
137 B.-Y. Chang and S.-M. Park, Electrochemical impedance spectroscopy, *Annu. Rev. Anal. Chem.*, 2010, **3**(1), 207–229.
138 A. C. Lazanas and M. I. Prodromidis, Electrochemical impedance spectroscopy–a tutorial, *ACS Meas. Sci. Au*, 2023, **3**(3), 162–193.
139 Q. Zhang, *et al.*, Investigation of structural evolution of $Li_{1.1}V3O8$ by in situ X-ray diffraction and density functional theory calculations, *Chem. Mater.*, 2017, **29**(5), 2364–2373.
140 C. Colinet and J.-C. Tedenac, Structural stability of the D8m-Ti5Sn2Si compound, *Calphad*, 2011, **35**(4), 643–647.
141 J. Ahn, *et al.* Verification of Strain-Induced Fast Ionic Conduction in Thin-Film Electrolyte Via Experimental and Computational Study. in Electrochemical Society Meeting Abstracts 233. 2018. The Electrochemical Society, Inc.
142 J. I.-z Chen and Q. Li, Advanced Materials And Energy Sustainability-Proceedings Of The 2016 International Conference On Advanced Materials And Energy Sustainability (Ames2016). 2017: World Scientific.
143 J. Halldin Stenlid and J. W. Lawson. Atomic-Scale Modeling of Charge-Transfer Kinetics at LixCoO2 Cathode-Electrolyte Interfaces. in Electrochemical Society Meeting Abstracts 245. 2024. The Electrochemical Society, Inc.
144 S. Huang, P. Verma and D. G. Truhlar, Localizing holes as polarons and predicting band gaps, defect levels, and delithiation energies of solid-state materials with a local exchange-correlation functional, *J. Phys. Chem. C*, 2017, **121**(43), 23955–23963.
145 S. Falletta and A. Pasquarello, Hubbard U through polaronic defect states, *npj Comput. Mater.*, 2022, **8**(1), 263.
146 A. Janotti and C. G. Van de Walle, LDA+ U and hybrid functional calculations for defects in ZnO, SnO2, and TiO2, *Phys. Status Solidi B*, 2011, **248**(4), 799–804.
147 M. Yu, *et al.*, Machine learning the Hubbard U parameter in DFT+U using Bayesian optimization, *npj Comput. Mater.*, 2020, **6**(1), 180.
148 M. Mendelev and D. Srolovitz, Impurity effects on grain boundary migration, *Modell. Simul. Mater. Sci. Eng.*, 2002, **10**(6), R79.
149 C. Freysoldt, *et al.*, Limitations of empirical supercell extrapolation for calculations of point defects in bulk, at surfaces, and in two-dimensional materials, *Phys. Rev. B*, 2022, **105**(1), 014103.
150 C. Hu, R. Dingreville and B. L. Boyce, Computational modeling of grain boundary segregation: A review, *Comput. Mater. Sci.*, 2024, **232**, 112596.
151 J. A. Dawson, Going against the grain: atomistic modeling of grain boundaries in solid electrolytes for solid-state batteries, *ACS Mater. Au*, 2023, **4**(1), 1–13.
152 K. Koester and P. Kaghazchi. Advanced Ab Initio Simulations of Layered Oxide Cathodes: Screening Atomistic Arrangements and Accurate Electronic Structures. in Electrochemical Society Meeting Abstracts prime2024. 2024. The Electrochemical Society, Inc.
153 E. Ertekin, *et al.*, Interplay between intrinsic defects, doping, and free carrier concentration in $SrTiO_3$ thin films, *Phys. Rev. B:Condens. Matter Mater. Phys.*, 2012, **85**(19), 195460.
154 K. Ghuman Understanding the Impact of Defects and Disorder in Materials for Advanced Energy Devices. in

Electrochemical Society Meeting Abstracts prime2024. 2024. The Electrochemical Society, Inc.
155 M. Weidner, *et al.*, Defect modulation doping, *Adv. Funct. Mater.*, 2019, **29**(14), 1807906.
156 D. Morgan, *et al.* Descriptors, Defects, and DFT for Solid Oxide Fuel Cell Materials. in Electrochemical Society Meeting Abstracts 231. 2017. The Electrochemical Society, Inc.
157 P. Ganesh Functional Defects By Design—a High-Throughput Approach to Energy Materials Discovery. in Electrochemical Society Meeting Abstracts 236. 2019. The Electrochemical Society, Inc.
158 M. Choi, *et al.*, Geometrical doping at the atomic scale in oxide quantum materials, *ACS Nano*, 2023, **17**(15), 14814–14821.
159 L. Weston, First-Principles Theoretical Studies of Bulk, Defect and Interface Properties of Oxide Semiconductors. 2015.
160 N. Filipoiu, *et al.*, Impact of interface defects on the band alignment and performance of TiO_2/MAPI/Cu_2O perovskite solar cells, *arXiv*, 2024, preprint, arXiv:2406.19594, DOI: 10.48550/arxiv.2406.19594.
161 F. Oba, *et al.*, Theoretical and data-driven approaches to semiconductors and dielectrics: from prediction to experiment, *Sci. Technol. Adv. Mater.*, 2024, **25**(1), 2423600.
162 A. Barman, *et al.*, Aliovalent Ta-Doping-Engineered Oxygen Vacancy Configurations for Ultralow-Voltage Resistive Memory Devices: A DFT-Supported Experimental Study, *ACS Appl. Mater. Interfaces*, 2022, **14**(30), 34822–34834.
163 J. Petropoulos, *et al.*, A simple thermodynamic model for the doping and alloying of nanoparticles, *Nanotechnology*, 2011, **22**(24), 245704.
164 J. G. Kim, *et al.*, Back Cover: Zr4+ Doping in Li4Ti5O12 Anode for Lithium-Ion Batteries: Open Li+ Diffusion Paths through Structural Imperfection (ChemSusChem 5/2014), *ChemSusChem*, 2014, **7**(5), 1490.
165 R. S. Ledwaba and P. E. Ngoepe. Enhanced Lithium Ion Diffusivity of Nanosized Li1. 2Mn0. 8O2 Cathode Material Via Na and Ti Co-Doping. in Electrochemical Society Meeting Abstracts 244. 2023. The Electrochemical Society, Inc.
166 A. A. Afashagov, M. A. Shebzukhova and A. Shebzukhov, Thermodynamic characteristics of the interface between condensed phases in binary metal alloys, *Phys. Solid State*, 2022, **64**(6), 293–299.
167 X. Long, *et al.*, Collaborative role of co-doping and surface modifying for adjusting surface state of hematite to release the photoelectrochemical activity, *J. Alloys Compd.*, 2024, **991**, 174235.
168 V. A. Sadykov, *et al.*, Ni-loaded nanocrystalline ceria-zirconia solid solutions prepared via modified Pechini route as stable to coking catalysts of CH4 dry reforming, *Open Chem.*, 2016, **14**(1), 363–376.
169 S. Breuer, M. Uitz and H. Wilkening, Rapid Li ion dynamics in the interfacial regions of nanocrystalline solids. The, *J. Phys. Chem. Lett.*, 2018, **9**(8), 2093–2097.
170 G. K. P. Dathar, *et al.*, Calculations of Li-ion diffusion in olivine phosphates, *Chem. Mater.*, 2011, **23**(17), 4032–4037.
171 J. Hur, Nanomaterials for ion battery applications, *Nanomaterials*, 2022, 2293.
172 M. S. R. Limon and Z. Ahmad, Heterogeneity in Point Defect Distribution and Mobility in Solid Ion Conductors, *ACS Appl. Mater. Interfaces*, 2024, **16**(38), 50948–50960.
173 H. Jena and H. Mainz, *Phys. Rev. B*, 2025, **111**, 174111.
174 A. L. Zand, *et al.*, Influence of defects on enhancing lithium diffusivity in crystalline silicon anodes for fast charging lithium-ion batteries, *J. Power Sources*, 2024, **606**, 234557.
175 K. Yang, L. Hong and M. Tang. Defect-Enhanced Phase Transformation Kinetics in Intercalation Compounds. in Electrochemical Society Meeting Abstracts 235. 2019. The Electrochemical Society, Inc.
176 A. Vasileiadis, Modeling Electrode Materials.
177 A.-d Dompablo, A. Morales-García and M. Taravillo, DFT+U calculations of crystal lattice, electronic structure, and phase stability under pressure of TiO2 polymorphs, *J. Chem. Phys.*, 2011, **135**(5), 054503.
178 S. Lutfalla, V. Shapovalov and A. T. Bell, Calibration of the DFT/GGA+ U method for determination of reduction energies for transition and rare earth metal oxides of Ti, V, Mo, and Ce, *J. Chem. Theory Comput.*, 2011, **7**(7), 2218–2223.
179 Q. T. Trinh, *et al.*, Synergistic application of XPS and DFT to investigate metal oxide surface catalysis, *J. Phys. Chem. C*, 2018, **122**(39), 22397–22406.
180 M. Capdevila-Cortada, Z. Łodziana and N. López, Performance of DFT+U approaches in the study of catalytic materials, *ACS Catal.*, 2016, 8370–8379.
181 Z. Wang, *et al.*, Tuning the crystal and electronic structure of Li4Ti5O12 via Mg/La Co-doping for fast and stable lithium storage, *Ceram. Int.*, 2020, **46**(9), 12965–12974.
182 H. S. Bhatti, *et al.*, Effects of cobalt doping on structural, optical, electrical and electrochemical properties of Li4Ti5O12 anode, *J. Alloys Compd.*, 2022, **890**, 161691.
183 Z. Su, Defect engineering on inorganic oxides for Lithium-ion batteries. 2021.
184 U. V. Kawade, *et al.*, Surface modified $Li_4Ti_5O_{12}$ by paper templated approach for enhanced interfacial Li+ charge transfer in Li-ion batteries, *RSC Adv.*, 2018, **8**(67), 38391–38399.
185 T. Vegge Electrochemical Interfaces in Energy Storage: Theory Meets Experiment. in Electrochemical Society Meeting Abstracts 244. 2023. The Electrochemical Society, Inc.
186 H. M. You, *et al.*, Atomistic scale modeling of anode/electrolyte interfaces in Li-Ion batteries, *Langmuir*, 2024, **40**(4), 1961–1970.
187 J. Qi, Insights Into Solid Electrolytes From Long-Time and Large-Size Scale Simulations With Machine Learning Interatomic Potentials. 2024, University of California, San Diego.
188 N. Takenaka, *et al.*, Frontiers in theoretical analysis of solid electrolyte interphase formation mechanism, *Adv. Mater.*, 2021, **33**(37), 2100574.
189 C. Cheng, *et al.*, Dynamic Molecular Investigation of the Solid-Electrolyte Interphase of an Anode-Free Lithium Metal Battery Using In Situ Liquid SIMS and Cryo-TEM, *Nano Lett.*, 2023, **23**(18), 8385–8391.

190 R. Cappabianca, *et al.*, An overview on transport phenomena within solid electrolyte interphase and their impact on the performance and durability of lithium-ion batteries, *Energies*, 2023, **16**(13), 5003.
191 M. Bin Jassar, *et al.*, A Perspective on the Molecular Modeling of Electrolyte Decomposition Reactions for Solid Electrolyte Interphase Growth in Lithium-Ion Batteries, *Adv. Funct. Mater.*, 2024, **34**(30), 2313188.
192 M. Morey, M. Lobel and E. Ryan. Simulation of the Solid Electrolyte Interphase Layer in Lithium Metal Batteries–a Systematic Study. in Electrochemical Society Meeting Abstracts prime2024. 2024. The Electrochemical Society, Inc.
193 S. Perez Beltran and P. B. Balbuena. Unraveling the Dynamics of Solid–Electrolyte Interphase (SEI) Formation on Lithium Metal: Insights from Multiscale Modeling. in Electrochemical Society Meeting Abstracts 245. 2024. The Electrochemical Society, Inc.
194 Y.-B. He, *et al.*, Effect of solid electrolyte interface (SEI) film on cyclic performance of Li4Ti5O12 anodes for Li ion batteries, *J. Power Sources*, 2013, **239**, 269–276.
195 M. M. Mandurah, *et al.*, Dopant segregation in polycrystalline silicon, *J. Appl. Phys.*, 1980, **51**(11), 5755–5763.
196 V. Jafarova and G. Orudzhev, Structural and electronic properties of ZnO: A first-principles density-functional theory study within LDA (GGA) and LDA (GGA)+ U methods, *Solid State Commun.*, 2021, **325**, 114166.
197 S. C. Pandey, *et al.*, Electronic and vibrational properties of transition metal-oxides: Comparison of GGA, GGA+ U, and hybrid approaches, *Chem. Phys. Lett.*, 2017, **669**, 1–8.
198 J. Kim, *et al.*, Accelerating the search for new solid electrolytes: exploring vast chemical space with machine learning-enabled computational calculations, *ACS Appl. Mater. Interfaces*, 2023, **15**(45), 52427–52435.
199 B. Zhang, *et al.*, Revolutionizing chemistry and material innovation: an iterative theoretical-experimental paradigm leveraged by robotic AI chemists, *CCS Chem.*, 2025, **7**(2), 345–360.
200 K. Boonpalit, J. Kinchagawat and S. Namuangruk, Expanding the applicability domain of machine learning model for advancements in electrochemical material discovery, *ChemElectroChem*, 2024, **11**(10), e202300681.
201 C. Duan, *et al.*, Learning from failure: predicting electronic structure calculation outcomes with machine learning models, *J. Chem. Theory Comput.*, 2019, **15**(4), 2331–2345.
202 I. Tanaka, Data-Driven Materials Discovery from Large Chemistry Spaces, *Matter*, 2020, **3**(2), 327–328.
203 H. Chan, *et al.*, Machine learning classical interatomic potentials for molecular dynamics from first-principles training data, *J. Phys. Chem. C*, 2019, **123**(12), 6941–6957.
204 H. Sun, *et al.*, Molecular dynamics simulation of Fe-Si alloys using a neural network machine learning potential, *Phys. Rev. B*, 2023, **107**(22), 224301.
205 R. Martin-Barrios, *et al.*, An overview about neural networks potentials in molecular dynamics simulation, *Int. J. Quantum Chem.*, 2024, **124**(11), e27389.
206 İ. C. Dikmen, N. Yildiran and T. Karadag, Machine Learning Approaches for Enhancing the SoH Estimation of LTO Batteries, *Int. J. Automot. Sci. Technol.*, 2025, **9**(1), 48–59.
207 C. Lv, *et al.*, Machine learning: an advanced platform for materials development and state prediction in lithium-ion batteries, *Adv. Mater.*, 2022, **34**(25), 2101474.
208 I. Can Dikmen, N. Yıldıran and T. Karadağ, Machine Learning Approaches for Enhancing the SoH Estimation of LTO Batteries, *Int. J. Automot. Sci. Technol.*, 2025, **9**, 1.
209 G. Armstrong, *et al.*, TiO2 (B) nanowires as an improved anode material for lithium-ion batteries containing LiFePO4 or LiNi0. 5Mn1. 5O4 cathodes and a polymer electrolyte, *Adv. Mater.*, 2006, **18**(19), 2597–2600.
210 A. Majid, *et al.*, A DFT study on nano-voids enhanced lithium storage capacity in Li4Ti5O12 anodes for lithium-ion batteries, *Mater. Sci. Semicond. Process.*, 2026, **203**, 110211.
211 E. B. Khan, *et al.* Analyzing Ad Exposure and Content in Child-Oriented Videos on YouTube. in Proceedings of the ACM Web Conference 2024. 2024.
212 H. Guo, *et al.*, Accelerated atomistic modeling of solid-state battery materials with machine learning, *Front. Energy Res.*, 2021, **9**, 695902.
213 S. T. Kelly, *et al.* Fueling the Simulation Machine: Considerations for High-Resolution 3D Microscopy to Support Computational Modeling in Battery Research. in Electrochemical Society Meeting Abstracts 242. 2022. The Electrochemical Society, Inc.
214 A. Sanin, J. K. Flowers and H. S. Stein. Combining High-Throughput Electrochemistry and Data-Driven Experimentation for Digital Discovery of Si-Ge-Sn Thin-Film Battery Anode Materials. in Electrochemical Society Meeting Abstracts prime2024. 2024. The Electrochemical Society, Inc.
215 N. Onofrio, M. Hellström and P. Spiering. Leverage Battery Research with Atomistic Modeling and Machine Learning. in Electrochemical Society Meeting Abstracts prime2024. 2024. The Electrochemical Society, Inc.
216 Z. Zhao, *et al.*, Deep learning-driven evaluation and prediction of ion-doped NASICON materials for enhanced solid-state battery performance, *AAPPS Bull.*, 2024, **34**(1), 26.
217 G. Hua, Y. Fan and Q. Zhang, Application of computational simulation on the study of lithium metal anodes, *Acta Phys.-Chim. Sin.*, 2021, **37**(2), 2008089.
218 K. Smith Simulation of Battery Chemo-Mechanical Physics Incorporating Degradation. in Electrochemical Society Meeting Abstracts 243. 2023. The Electrochemical Society, Inc.